

Supplementary Information for

**Mechanically-Robust All-Polymer Solar Cells Enabled by  
Polymerized Small Molecule Acceptors Featuring Flexible  
Siloxane-Spacers**

*Jin-Woo Lee,<sup>†,a</sup> Sun-Woo Lee,<sup>†,b</sup> Jingwan Kim,<sup>†,c</sup> Yeon Hee Ha,<sup>c</sup> Cheng Sun,<sup>c</sup> Tan Ngoc-Lan  
Phan,<sup>a</sup> Seungjin Lee,<sup>a</sup> Cheng Wang,<sup>d</sup> Taek-Soo Kim<sup>\*,b</sup> Yun-Hi Kim,<sup>\*,c</sup> and Bumjoon J. Kim<sup>\*,a</sup>*

<sup>a</sup> Department of Chemical and Biomolecular Engineering and <sup>b</sup> Mechanical Engineering, Korea  
Advanced Institute of Science and Technology (KAIST), Daejeon 34141, Republic of Korea

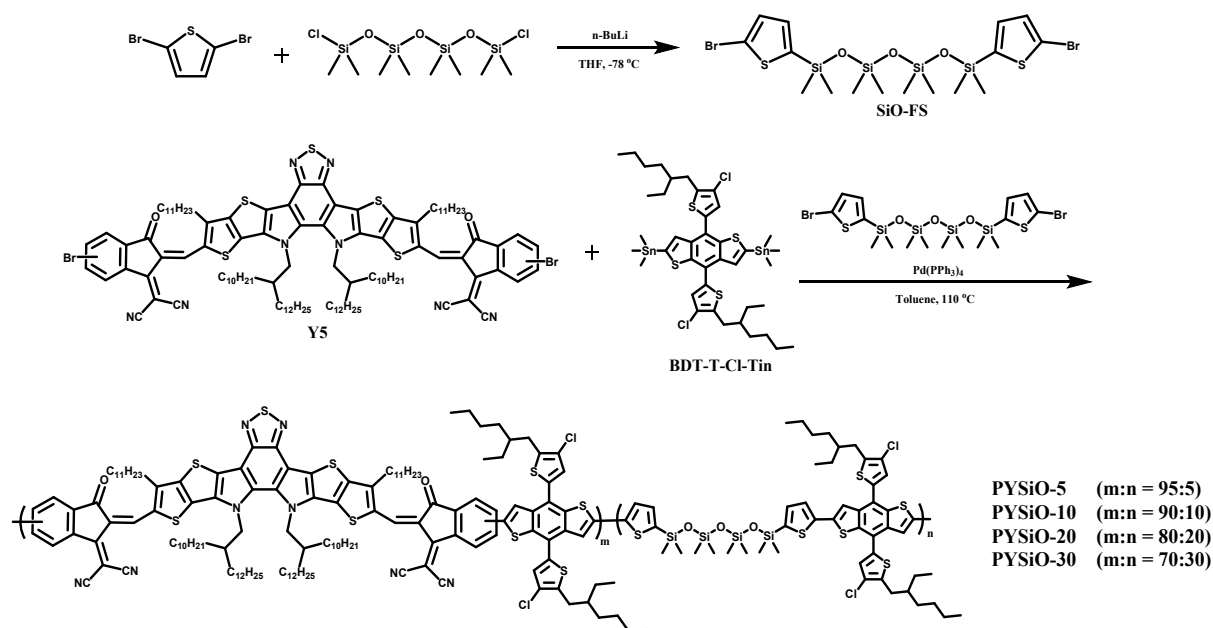
<sup>c</sup> Department of Chemistry and RINS, Gyeongsang National University, Jinju 52828, Republic  
of Korea

<sup>d</sup> Advanced Light Source, Lawrence Berkeley National Laboratory, 1 Cyclotron Road,  
Berkeley, CA 94720, United States

\*Electronic mail: [tskim1@kaist.ac.kr](mailto:tskim1@kaist.ac.kr), [ykim@gnu.ac.kr](mailto:ykim@gnu.ac.kr), and [bumjoonkim@kaist.ac.kr](mailto:bumjoonkim@kaist.ac.kr)

**Materials:** PBDB-T  $P_D$  was purchased from Brilliant Matters. All reagents and solvents were purchased from Aldrich, Alfa aesar and Tokyo chemical industry and used without further purification. Catalysts used in coupling reactions were purchased from Umicore. The Y5 monomer<sup>1</sup>, and BDT-T-Cl-Tin monomer<sup>2</sup> were synthesized by following the procedures in literature. The 2,9-bis(3-((3-(dimethylamino)propyl)amino)propyl)anthra[2,1,9-*def*:6,5,10-*d'e'f'*]diisoquinoline-1,3,8,10(2*H*,9*H*)-tetraone (PDINN) material was synthesized by following the method described in the literature.<sup>3</sup>

**Synthesis:**



crude product was isolated by column chromatography on silica gel using n-hexane as eluent to give a SiO-FS. (1.79 g, 72% yield).  $^1\text{H}$  NMR (300 MHz,  $\text{CD}_2\text{Cl}_2$ ,  $\delta$ ): 7.00 (d,  $J = 12$  Hz, 2H), 6.96 (d,  $J = 12$  Hz, 2H), 0.31 (s, 12H), 0.00 (s, 12H).  $^{13}\text{C}$  NMR (500 MHz,  $\text{CD}_2\text{Cl}_2$ ,  $\delta$ ): 142.63, 134.69, 131.14, 117.13, 1.34, 0.90. ESI-MS  $m/z$  calcd for  $\text{C}_{16}\text{H}_{28}\text{Br}_2\text{O}_3\text{S}_2\text{Si}_4$  ( $[\text{M}]^+$ ) 601.8924, found: 602.8925

**General procedure for the polymerization (PYSiO polymers)** : In a 25 mL Schlenk-Flask, compound Y5 (0.1080 to 0.1463 mmol), BDT-T-Cl-Tin (0.1540 mmol) and each SiO-FS (0.0462 to 0.0077 mmol) were dissolved in 15 mL of anhydrous toluene under nitrogen, respectively. The mixture was purged with nitrogen for 30 min, then  $\text{Pd}(\text{PPh}_3)_4$  (7.6 mg) was added in one portion. The oil bath was heated to 110 °C and the reactant was stirred for 48 h under argon atmosphere, respectively. After cooling down to the room temperature, the polymer solution was precipitated from methanol (200 mL). Subsequently, the resulting precipitate was collected by filtration and purified by Soxhlet extraction with methanol, acetone, hexane, dichloromethane, and chloroform in succession. The polymer was obtained as solid powder by precipitating in methanol.

**Synthesis of the PYSiO-5** : PYSiO-5 was polymerized with Y5 (0.2906 g, 0.1463 mmol), BDT-T-Cl-Tin (0.15 g, 0.1540 mmol) and SiO-FS (4.6 mg, 0.0077 mmol) by according to the general procedure. The polymer (Y5-BDT-T-4SiO-5%) was obtained as a black solid. (0.15 g, 40% yield).  $^1\text{H}$  NMR (500 MHz,  $\text{CDCl}_3$ ,  $\delta$ ): 9.5-7.3 (br, 11.8H), 5.2-4.4 (br, 3.8H), 3.5-3.2 (br, 7.8H), 2.0-0.5 (br, 159.2H) 0.5-0.3 (br, 0.6H), 0.2-0.0 (br, 0.6H).

**Synthesis of the PYSiO-10** : PYSiO-10 was polymerized with Y5 (0.2753 g, 0.1386 mmol), BDT-T-Cl-Tin (0.15 g, 0.1540 mmol) and SiO-FS (9.3 mg, 0.0154 mmol) by according to the general procedure. The polymer was obtained as a black solid. (0.28 g, 78% yield).  $^1\text{H}$  NMR (500 MHz,  $\text{CDCl}_3$ ,  $\delta$ ): 9.5-7.3 (br, 11.6H), 5.2-4.4 (br, 3.6H), 3.5-3.2 (br, 7.6H), 2.0-0.5 (br, 152.4H) 0.5-0.3 (br, 1.2H), 0.2-0.0 (br, 1.2H).

**Synthesis of the PYSiO-20** : PYSiO-20 was polymerized with Y5 (0.2447 g, 0.1232 mmol), BDT-T-Cl-Tin (0.15 g, 0.1540 mmol) and SiO-FS (18.6 mg, 0.0308 mmol) by according to the general procedure. The polymer was obtained as a black solid. (0.25 g, 74% yield).  $^1\text{H}$  NMR

(500 MHz, CDCl<sub>3</sub>, δ): 9.5-7.3 (br, 11.2H), 5.2-4.4 (br, 3.2H), 3.5-3.2 (br, 7.2H), 2.0-0.5 (br, 138.8H) 0.5-0.3 (br, 2.4H), 0.2-0.0 (br, 2.4H).

**Synthesis of the PYSiO-30 :** PYSiO-30 was polymerized with Y5 (0.2139 g, 0.1080 mmol), BDT-T-Cl-Tin (0.15 g, 0.1540 mmol) and SiO-FS (27.9 mg, 0.0462 mmol) by according to the general procedure. The polymer was obtained as a black solid. (0.22 g, 69% yield). <sup>1</sup>H NMR (500 MHz, CDCl<sub>3</sub>, δ): 9.5-7.3 (br, 10.8H), 5.2-4.4 (br, 2.8H), 3.5-3.2 (br, 6.8H), 2.0-0.5 (br, 125.2H) 0.5-0.3 (br, 3.6H), 0.2-0.0 (br, 3.6H).

**Characterizations:** <sup>1</sup>H NMR and <sup>13</sup>C NMR spectra were recorded with Advance 300 and DRX 500 MHz FT-NMR Bruker spectrometers, and chemical shifts (ppm) were reported with tetramethylsilane as an internal standard. High resolution mass analysis was obtained by a Joel JMS-700. UV-Vis spectra were measured by a Shimadzu Scientific Instruments UV-1800 spectrophotometer. Cyclic voltammetry (CV) measurements were obtained from a ZIVE SP1 Electrochemical at a scan rate of 10 mV s<sup>-1</sup>. *M<sub>n</sub>* and *D* of the polymers were obtained from an Agilent GPC 1200 series relative to polystyrene standards, using *ortho*-dichlorobenzene eluent at 80 °C. RSoXS measurements were proceeded at BL 11.0.1.2 in the Advanced Light Source (USA). GIXS profiles were measured at the beamline 3C at Pohang Accelerator Laboratory, Korea. The incidence angles were set to 0.12 – 0.14° for complete penetration of thin films. *L<sub>c</sub>* values of the polymer films were calculated by Scherrer equation.

$$L_c = \frac{2\pi K}{\Delta_q}$$

(*K*,  $\Delta_q$  = shape factor (0.9), full width at half maximum (FWHM) of scattered peaks, respectively.)

**All-PSC Fabrication:** The normal type all-PSCs (indium tin oxide (ITO)/ poly 3,4-ethylenedioxythiophene:polystyrene sulfonic acid (PEDOT:PSS, AI4083 from Heraeus)/active layer/PDINN/Ag) were fabricated by the following processes. ITO-coated glass substrates were treated with ultra-sonication by acetone and isopropyl alcohol solvents. The cleaned substrates were dried for more than 2 h at 80 °C in an oven. A plasma treatment was proceeded for 10 min before spin-casting PEDOT:PSS solution. The PEDOT:PSS solution was spin-casted at 3000 rpm for 30 s, then thermally annealed at 165 °C for 20 min in ambient condition. Then, the samples were carried to a nitrogen-filled glovebox. Next, the blend solutions with

optimal concentration (20 mg mL<sup>-1</sup>) and donor:acceptor weight ratio (1:1.2) were prepared in *ortho*-xylene (*o*-XY) with 4 vol% of 1-fluoronaphthalene (1-FN) additive. The solutions were stirred for at least 2 h at 100 °C before spin-coating. Then, the solutions were spin-casted onto the PEDOT:PSS-coated ITO substrates at 1700 rpm for 30 s, and the films were thermally annealed at 120 °C for 10 min. After that, the samples were dried at a high-vacuum chamber for 1 h. Then, the PDINN solution (1 mg mL<sup>-1</sup> in methanol) was spin-coated onto the active layer films with 3000 rpm for 30 s. Finally, Ag electrode (120 nm) was deposited by thermal evaporation in an evaporation chamber, under high vacuum (~10<sup>-6</sup> Torr) condition. The photoactive area of the all-PSC devices is 0.09 cm<sup>2</sup>, measured from the optical microscopy.

***Flexible All-PSC Fabrication:*** The device structure of a flexible all-PSC was thermoplastic urethane (TPU)/PH1000/AI4083/active layer/PDINN/Ag. PEDOT:PSS (Heraeus Clevios™ PH1000) containing 5 vol% of dimethyl sulfoxide (DMSO), 2 vol% polyethylene glycol (PEG), and 0.5 vol% of Zonyl fluorosurfactant (Zonyl FS-30) as dopants was stirred overnight prior to use. In details, DMSO was incorporated for improved electrical conductivity of PH1000 PEDOT:PSS, PEG for better mechanical property in stretchability, and Zonyl FS-30 for enhanced surface wettability. The PH1000 film was treated with citric acid to enhance conductivity. The TPU substrates were treated with plasma for 10 min before spin-coating the PH1000 electrodes. The PH1000 solution was spin-casted on the TPU substrates with 2000 rpm in the ambient condition. Then, the substrates were annealed in 100 °C for 20 min. After that, the PH1000 was spin-coated and annealed again for the formation of double-layer electrode. Next, plasma treatment was done on the PH1000-coated TPU substrates for 45 s, and then 2 layers of PEDOT:PSS (Heraeus Clevios™ AI4083) were spin-coated onto that at 2500 rpm for 40 s. The remained steps for the formations of active layers, interlayers, and electrodes are same with the aforementioned procedures for the all-PSC devices.

***SCLC Measurement:*** The electron- and hole-only devices for the SCLC measurement have device architectures of ITO/ZnO/active layer/LiF/Al and ITO/PEDOT:PSS/active layer/Au, respectively. The semiconducting films were spin-casted in a nitrogen-filled glovebox, and the blend films were prepared in the same condition with all-PSC fabrication. Mott-Gurney equation was used to fit the *J-V* characteristics:

$$J_{SCL} = \frac{9}{8} \epsilon_0 \epsilon_r \mu (V^2 / L^3)$$

( $\epsilon_0$  = the free-space permittivity,  $\epsilon_r$  = the dielectric constant of the semiconductor,  $\mu$  = the mobility,  $V$  = the applied voltage, and  $L$  = the thickness of the active layer.)

***Pseudo-freestanding tensile test:*** In the pseudo free-standing tensile method, the films were prepared with the same condition with the all-PSC fabrications. The films were spin-casted onto the polystyrene sulfonic acid (PSS)-coated glass substrate, and cut into a dog-bone shape by a femtosecond laser. Then, the films were floated onto the water surface, and attached to the grips by van der Waals interactions. The strain was applied with a fixed strain rate ( $0.8 \times 10^{-3} \text{ s}^{-1}$ ), and the tensile load values were measured by a load cell with high resolution (LTS-10GA, KYOWA, Japan). Elastic modulus was calculated using least square method for the slope of the linear region in stress-strain curve within 0.5 % strain.

***In situ UV-Vis absorption measurement :*** The absorption spectra were examined using a HRR2000+CG spectrometer, equipped with DH-2000-BAL balanced deuterium tungsten light source. The OceanView spectroscopy software was applied for the measurements. The characterizations were performed with an integration time of 0.1 s.  $t_{\text{sat}}$  is defined as starting point of constant absorbance during spin-coating process, displaying quenched morphology in film state.

## Supplementary Figures and Tables

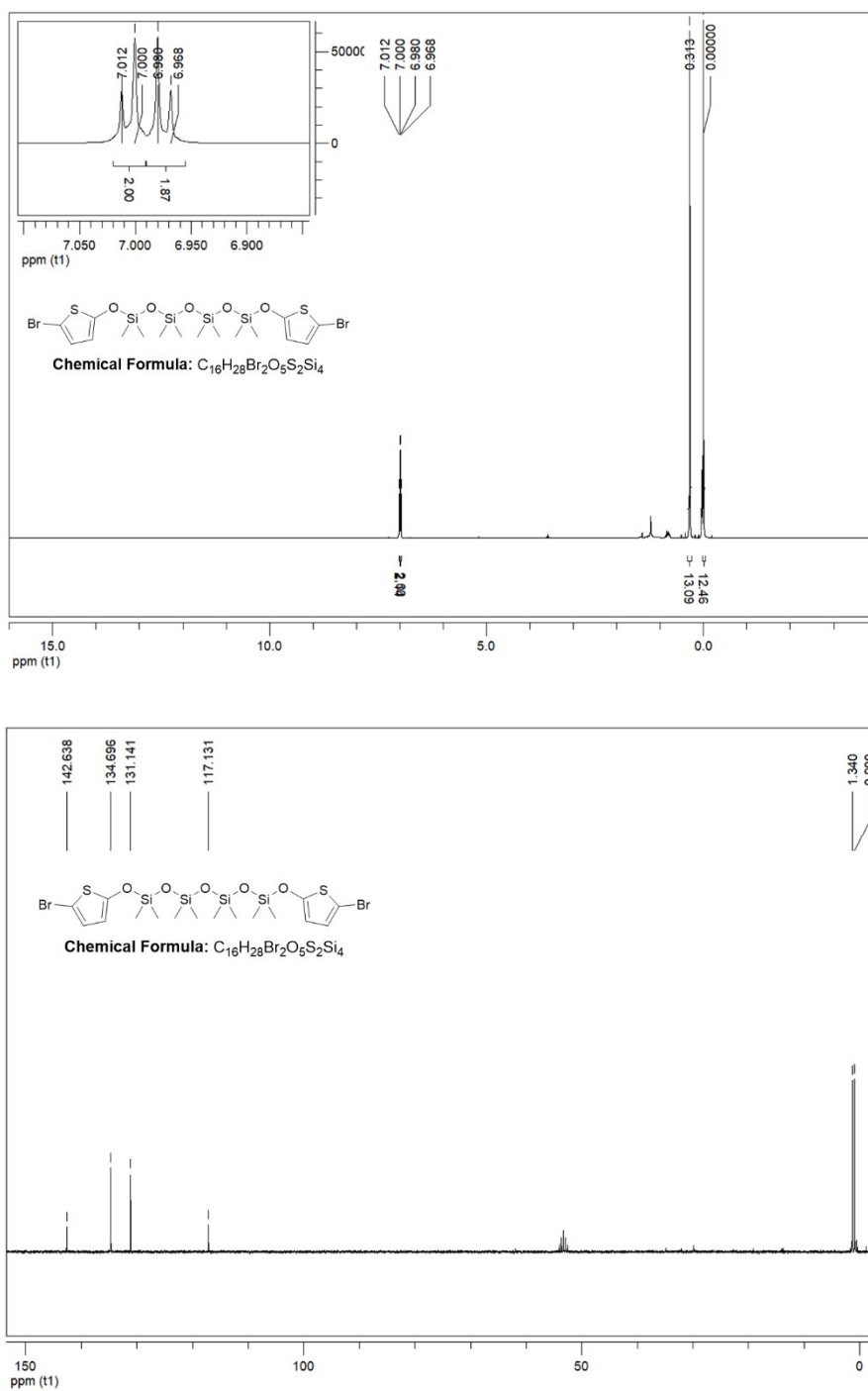


**Fig. S1.**  $^1H$ -NMR and  $^{13}C$ -NMR spectra of SiO-FS.

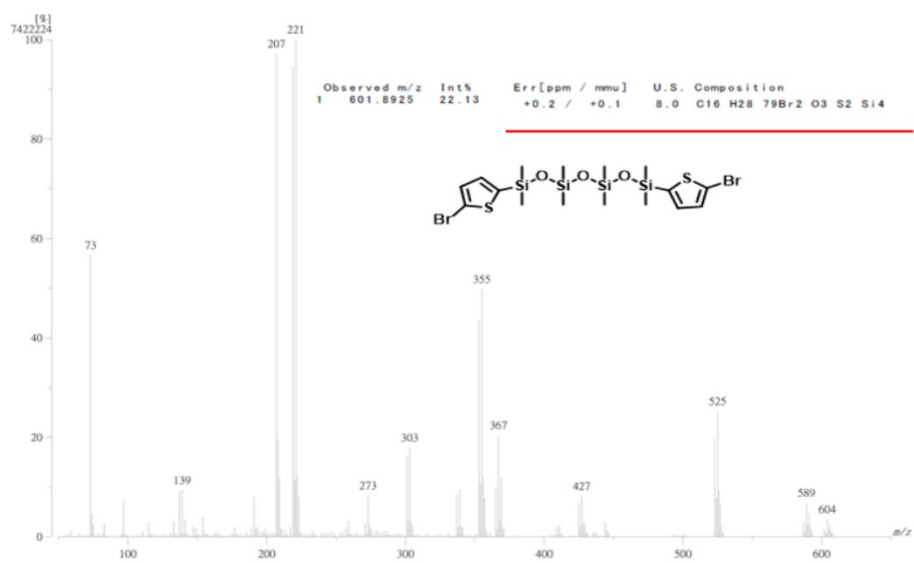
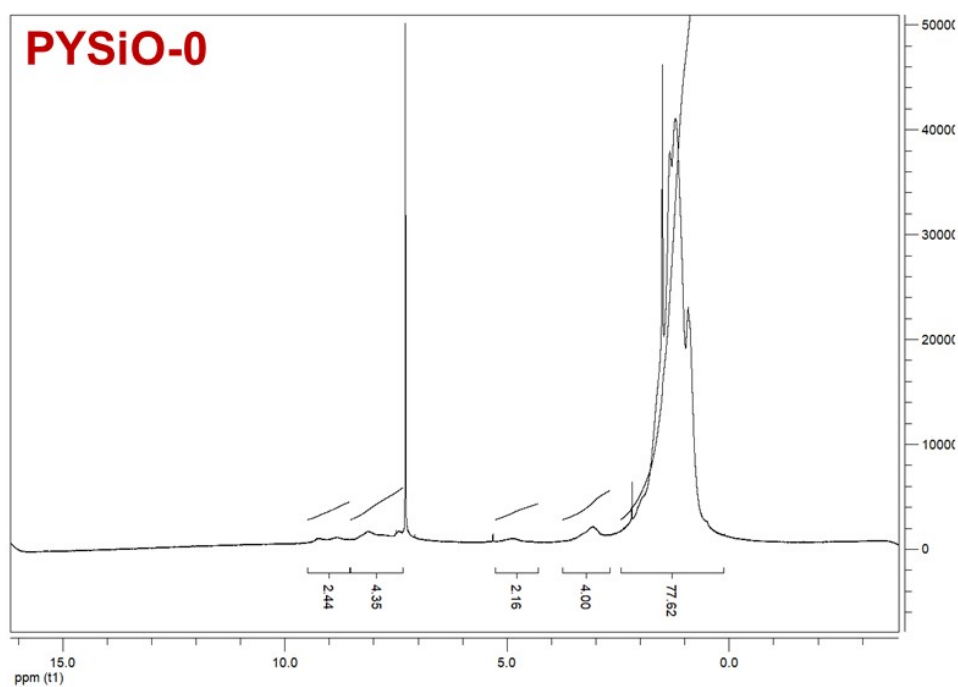
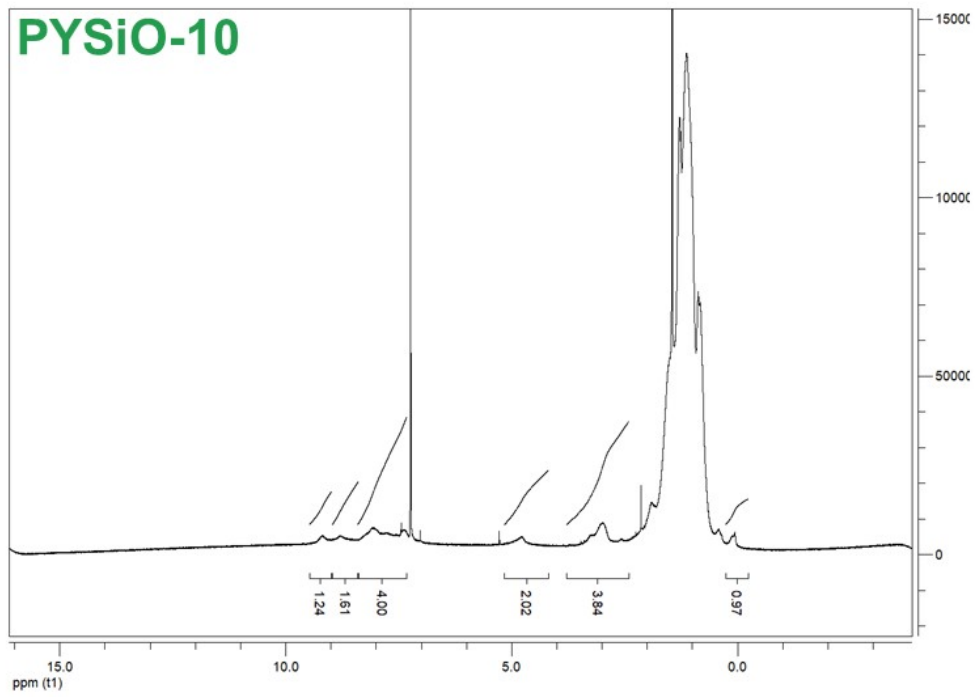
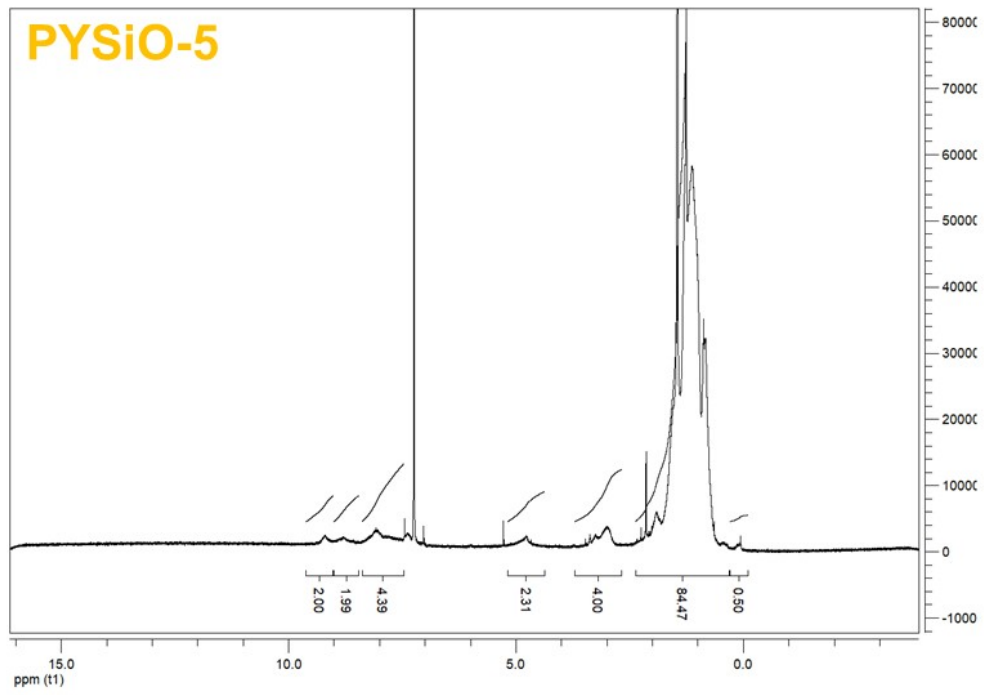
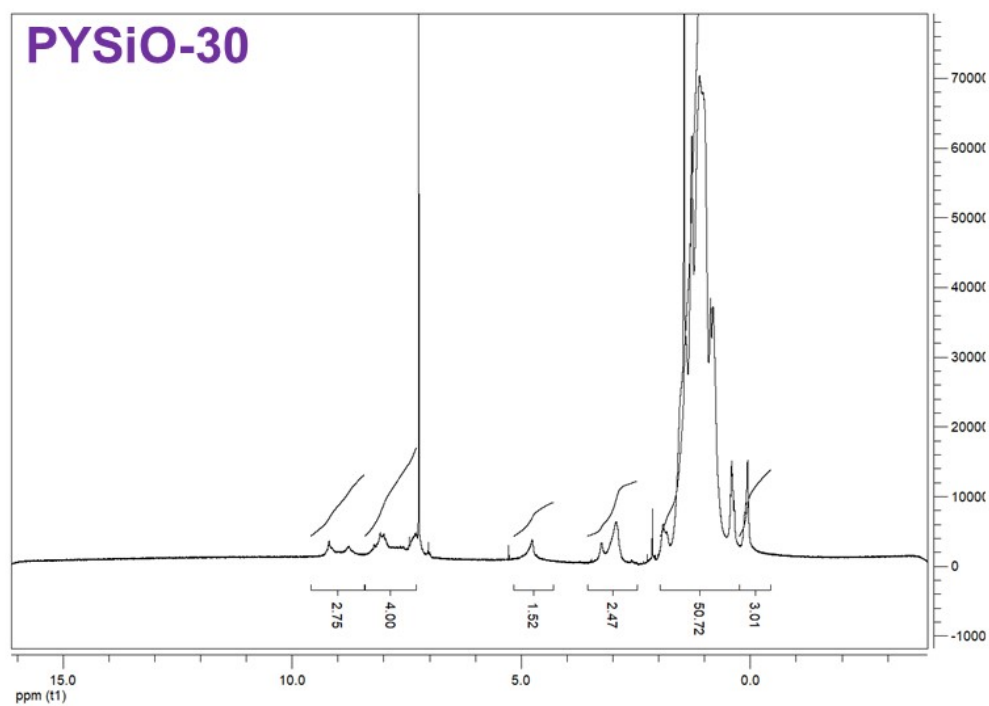
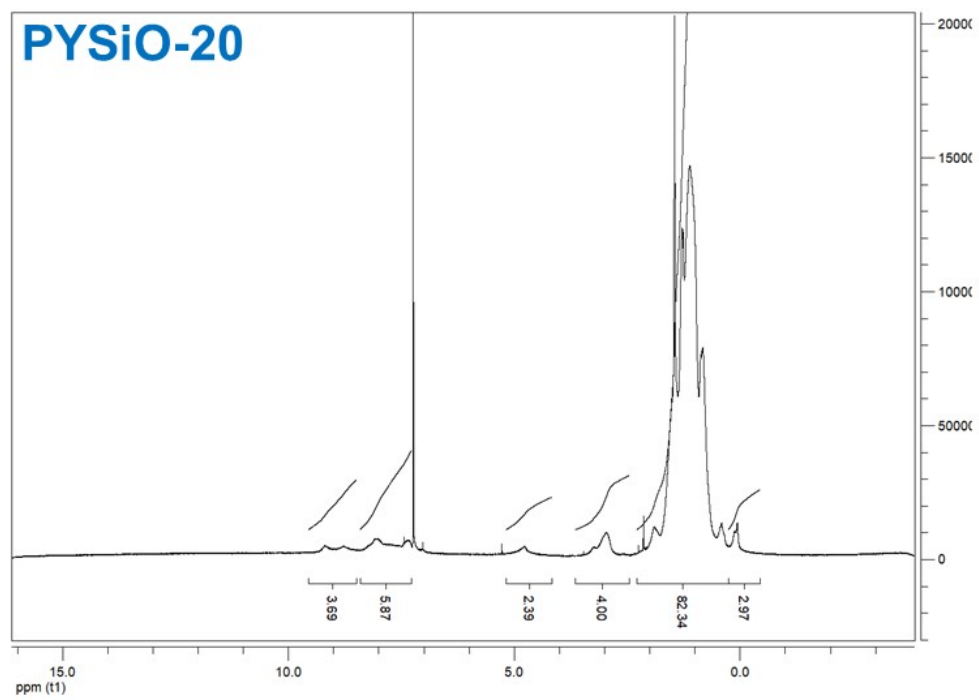


Fig. S2. MALDI-TOF spectra of SiO-FS.









**Fig. S3.** <sup>1</sup>H-NMR spectra of PYSiO-X PSMA.

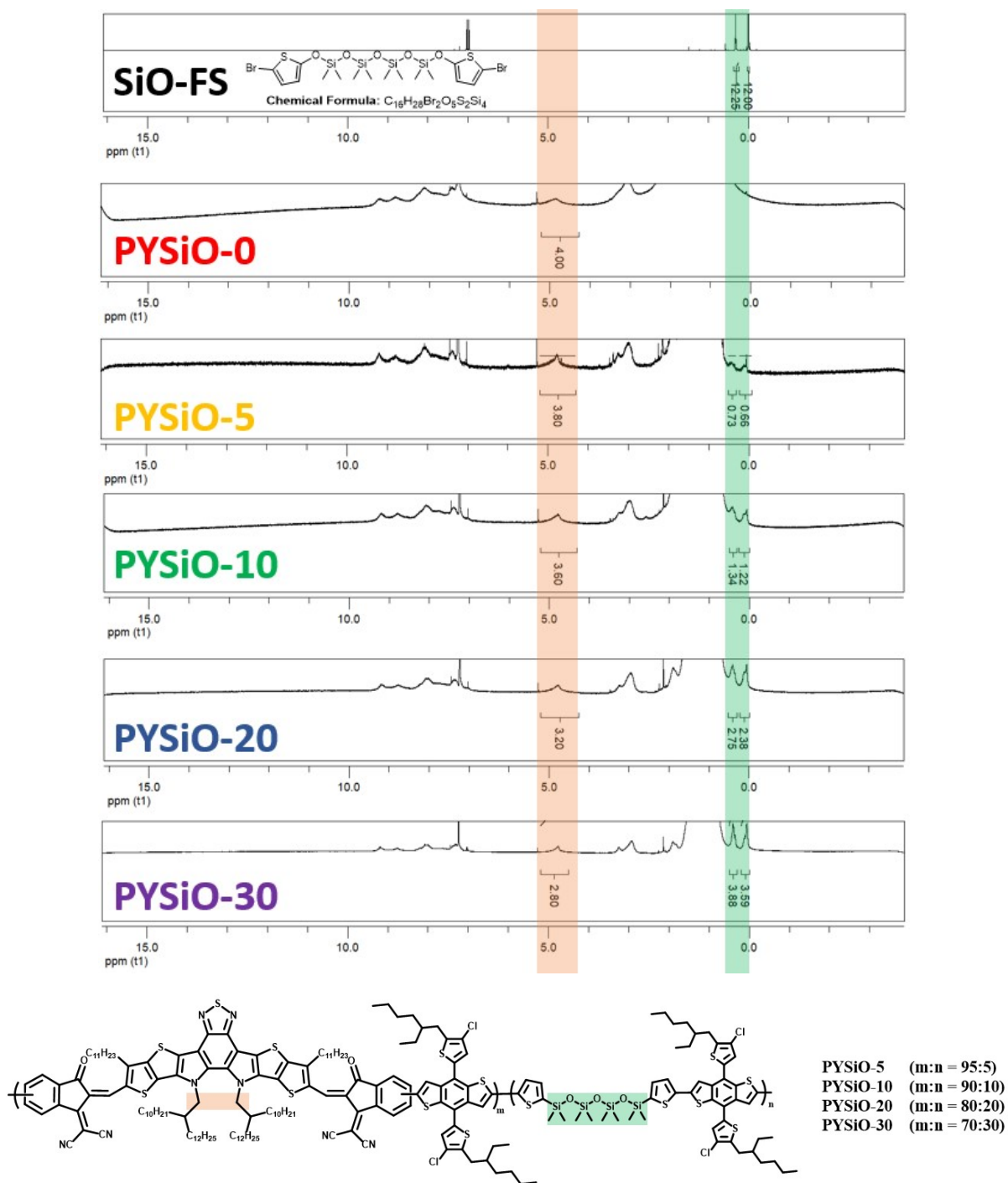


**Fig. S4.** Comparison of N-CH<sub>2</sub>-peak (5.2 – 4.3 ppm) and SiO peaks (0.7 – 0.0 ppm) in the <sup>1</sup>H-NMR of PYSiO-X P<sub>A</sub>S.

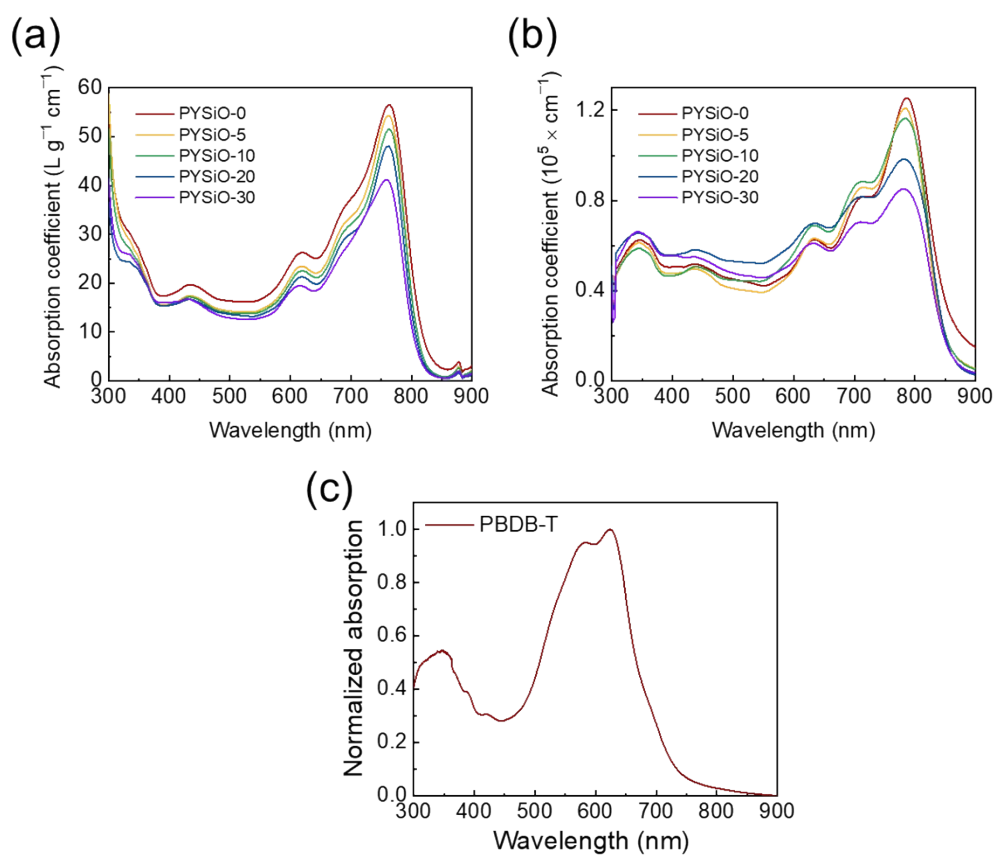


**Fig. S5.** Absorption coefficients of PSMA in (a) solution and (b) film states, and (c) normalized absorption of PBDB-T in film.

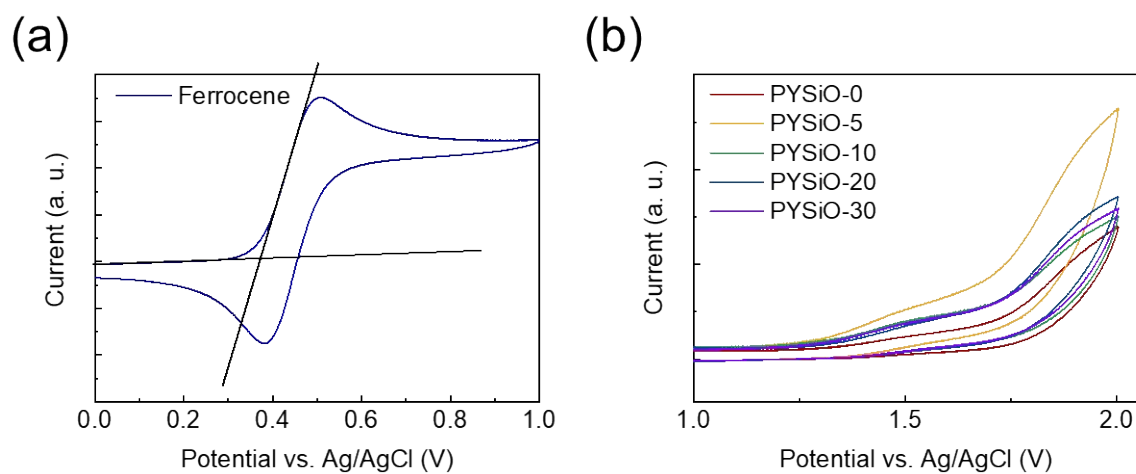


**Fig. S6.** CV profiles of (a) ferrocene and (b)  $P_A$  materials.

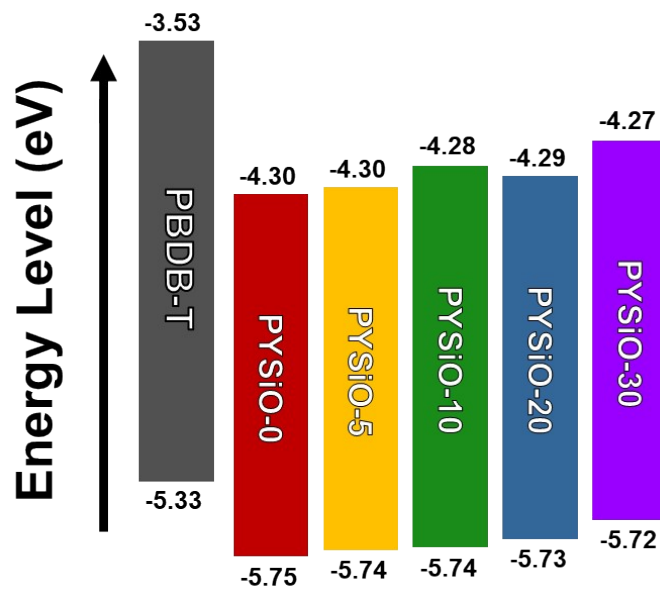


**Fig. S7.** Energy level alignments of the investigated materials.

**Table S1.** HOMO and LUMO energy levels of the investigated materials.

Polymer	HOMO (eV)	LUMO (eV)
PBDB-T	-5.33	-3.53
PYSiO-0	-5.75	-4.30
PYSiO-5	-5.74	-4.30
PYSiO-10	-5.74	-4.28
PYSiO-20	-5.73	-4.29
PYSiO-30	-5.72	-4.27

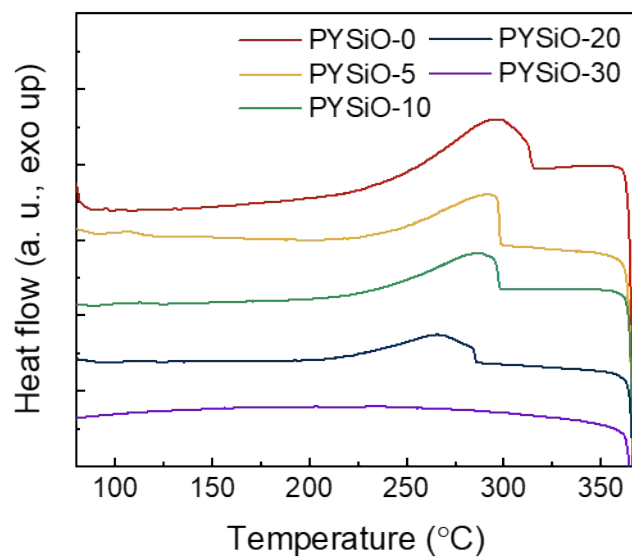


**Fig. S8.** DSC 2<sup>nd</sup> cooling cycles of PSMA with different SiO-FS contents.

**Table S2.** Thermal properties of PSMA obtained from DSC measurement.

Polymer	$T_m$ (°C) <sup>a</sup>	$\Delta H_m$ (J g <sup>-1</sup> ) <sup>a</sup>	$T_c$ (°C) <sup>b</sup>	$\Delta H_c$ (J g <sup>-1</sup> ) <sup>b</sup>
<b>PYSiO-0</b>	305	18.4	297	19.2
<b>PYSiO-5</b>	293	17.9	294	16.0
<b>PYSiO-10</b>	291	16.1	287	15.8
<b>PYSiO-20</b>	290	12.7	266	13.3
<b>PYSiO-30</b>	273	9.0	–	–

<sup>a</sup> Estimated from 2<sup>nd</sup> heating cycles. <sup>b</sup> Estimated from 2<sup>nd</sup> cooling cycles.

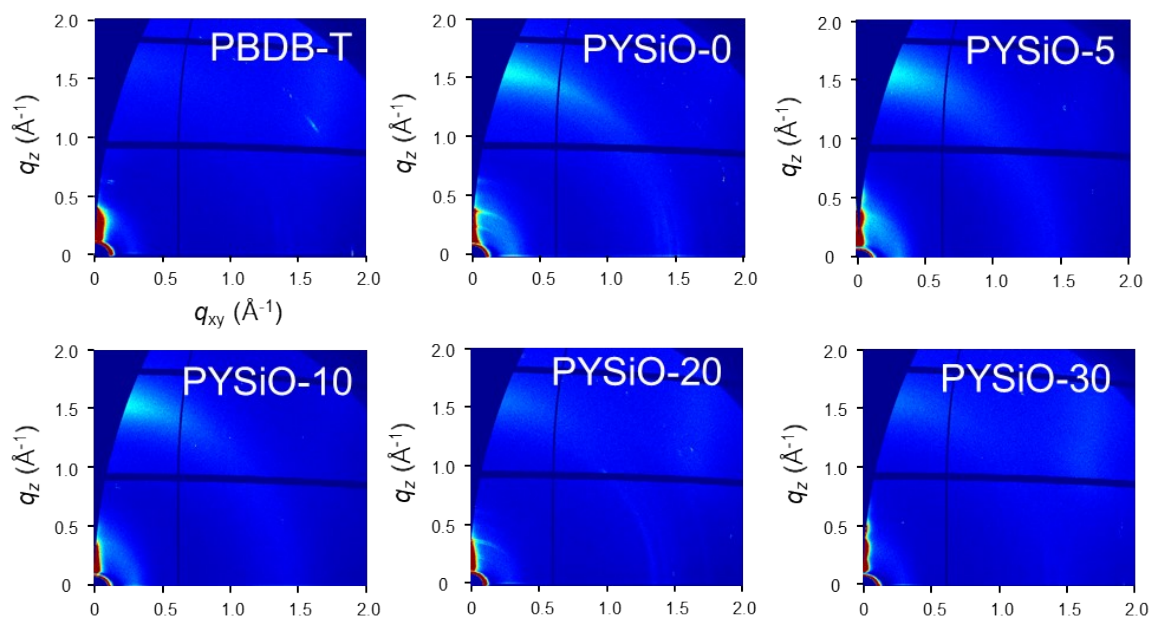


**Fig. S9.** 2D-images of the pristine films.

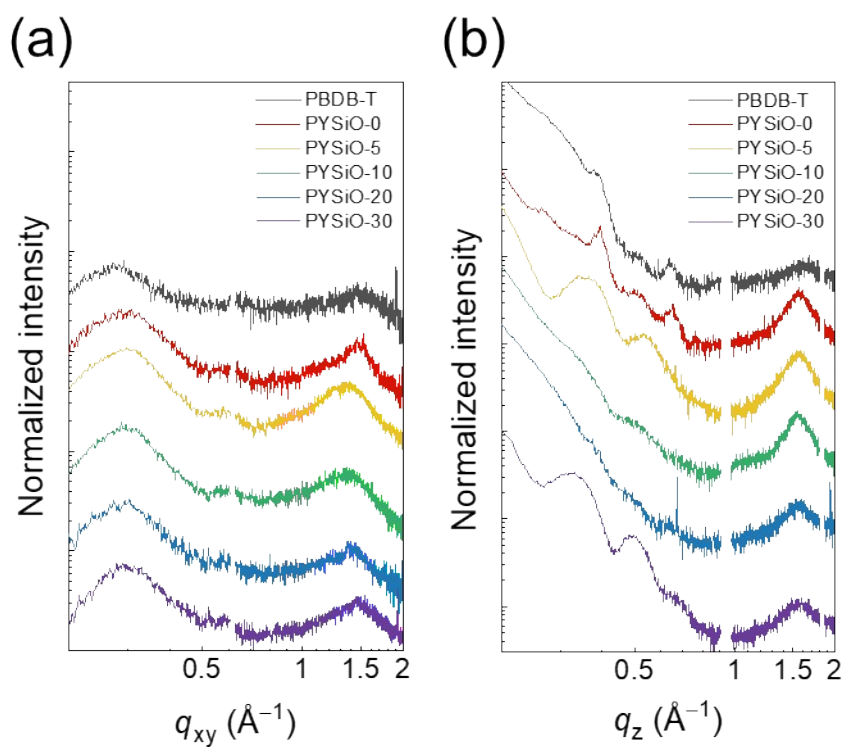


**Fig. S10.** GIXS linecut profiles of pristine films in the (a) IP and (b) OOP directions.

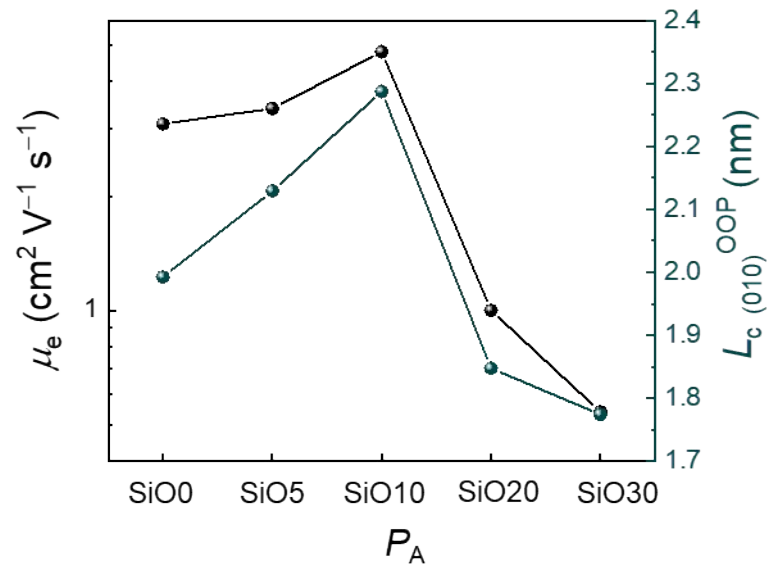


**Fig. S11.**  $\mu_e$  and  $L_{c(010)}^{\text{OOP}}$  plots of  $P_{AS}$  with different SiO-FS contents

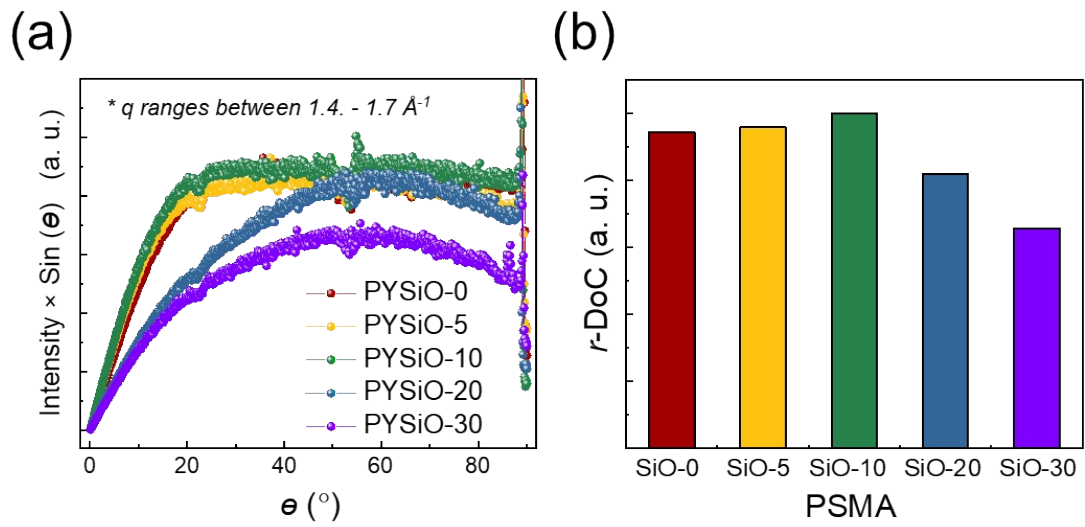


**Fig. S12.** (a) Intensity  $\times$   $\sin(\theta)$  and (b)  $r\text{-DoC}$  plots estimated from (010) peaks of the PSMAs.



**Table S3.** *r*-DoC values estimated from (010) peaks of the PSMA.

Polymer	<i>r</i> -DOC
PYSiO-0	0.94
PYSiO-5	0.96
PYSiO-10	1.00
PYSiO-20	0.82
PYSiO-30	0.66

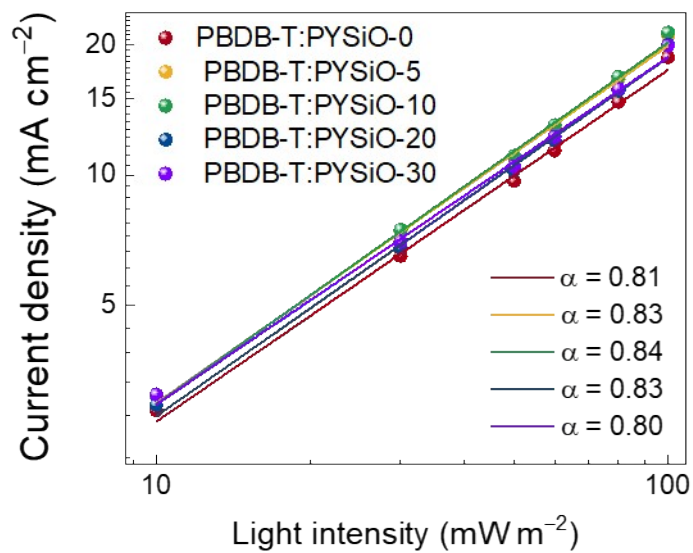


**Fig. S13.**  $J_{sc}$  plots as a function of light intensities of all-PSC blends.

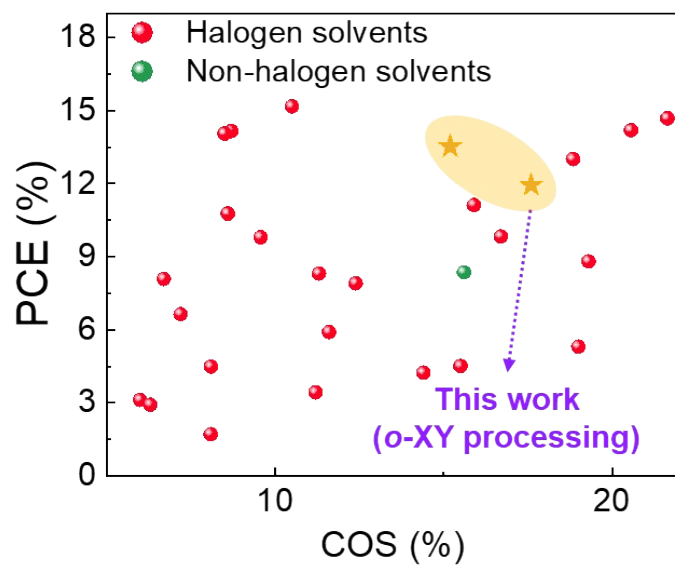


**Fig. S14.** Comparison of PCE and COS values of all-PSCs in reported works and this work.

**Table S4.** PSC PCE and COS measured by pseudo free-standing tensile tests in other works and this work.

Blend	Solvent	PCE <sub>max</sub> (%)	COS (%)	Reference
PBDTTTPD:P(NDI2HD-T)	Chloroform (CF)	6.64	7.2	4
PTB7-Th:P-15K	CF	3.12	6.0	5
PTB7-Th:P-20K	CF	3.43	11.2	5
PTB7-Th:P-48K	CF	4.24	14.4	5
PTB7-Th:P(NDI2HD-T)	Chlorobenzene (CB)	5.91	11.6	6
PTzBI:N2200	Methyl-tetrahydrofuran	8.36	15.6	7
PTzBI:N2200	CF	4.49	8.1	7
PTzBI:N2200	CB	2.92	6.3	7
J52:N2200	CF	5.30	19	8
PBZ-2Si <sub>L</sub> :N2200	CF	4.51	15.5	8
PBZ-2Si <sub>M</sub> :N2200	CF	6.89	38.1	8
PBZ-2Si <sub>H</sub> :N2200	CF	6.28	50.2	8
PM6:PF2-DTC	CF	8.31	11.3	9
PM6:PF2-DTSi	CF	10.77	8.6	9
PM6:PF2-DTGe	CF	8.09	6.7	9
PBDB-T:P(BDT2BOY5-H)	<i>ortho</i> -dichlorobenzene ( <i>o</i> -DCB)	8.81	19.3	10
PBDB-T:P(BDT2BOY5-F)	<i>o</i> -DCB	9.83	16.7	10
PBDB-T:P(BDT2BOY5-Cl)	<i>o</i> -DCB	11.12	15.9	10
PBDB-T:PY-O	CF	9.80	9.57	11
PBDB-T:PY-S	CF	14.16	8.70	11
PBDB-T:PYTS-0.0	CB	13.01	18.84	12
PBDB-T:PYTS-0.1	CB	14.19	20.56	12
PBDB-T:PYTS-0.3	CB	14.68	21.64	12
PBDB-T:PYTS-0.5	CB	7.91	12.39	12
PBDB-T:PYTS-1.0	CB	1.71	8.09	12
PBDB-T:PY-T (BHJ)	CF	14.06	8.5	13
PBDB-T:PY-T (LBL)	CF	15.17	10.5	13
PBDB-T:PYSiO-10	<i>o</i> -XY	13.52	15.2	<b>This work</b>

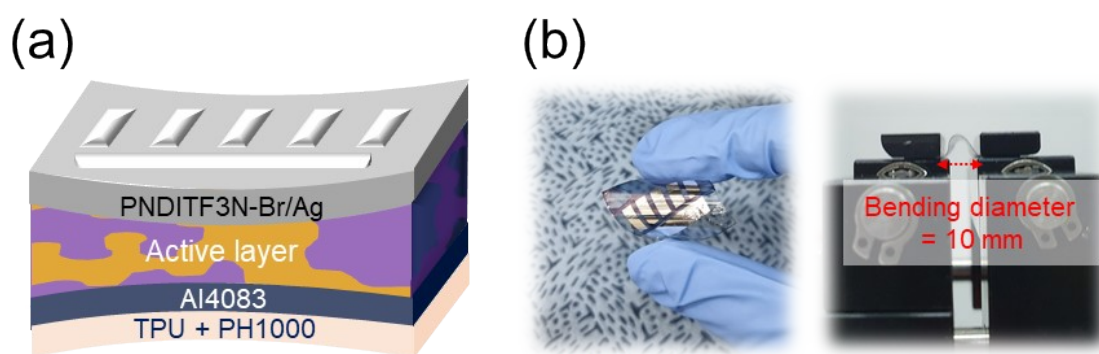


**Fig. S15.** (a) Device architecture, and (b) photographs of flexible all-PSCs.

**Table S5.** Photovoltaic performances of flexible all-PSCs.

$P_A$	$V_{oc}$ (V)	$J_{sc}$ ( $\text{mA cm}^{-2}$ )	FF	$\text{PCE}_{\max}$ (avg) <sup>a</sup> (%)
<b>PYSiO-0</b>	0.91	16.31	0.59	8.75 (8.48)
<b>PYSiO-10</b>	0.91	17.78	0.62	10.03 (9.68)

<sup>a</sup>Average values measured from more than 3 devices.

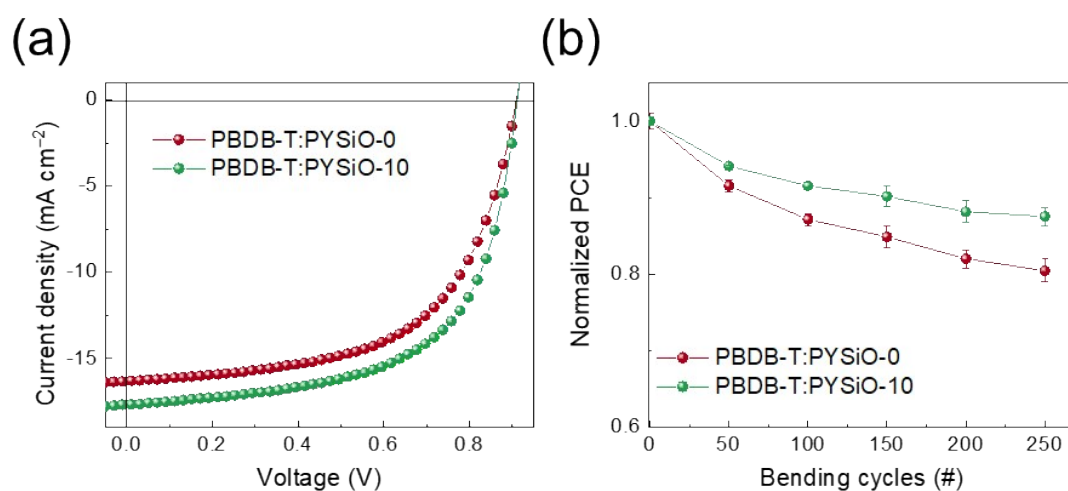


**Fig. S16.** (a)  $J$ - $V$  curves and (b) normalized PCE plots as a function of bending cycles of flexible all-PSCs.

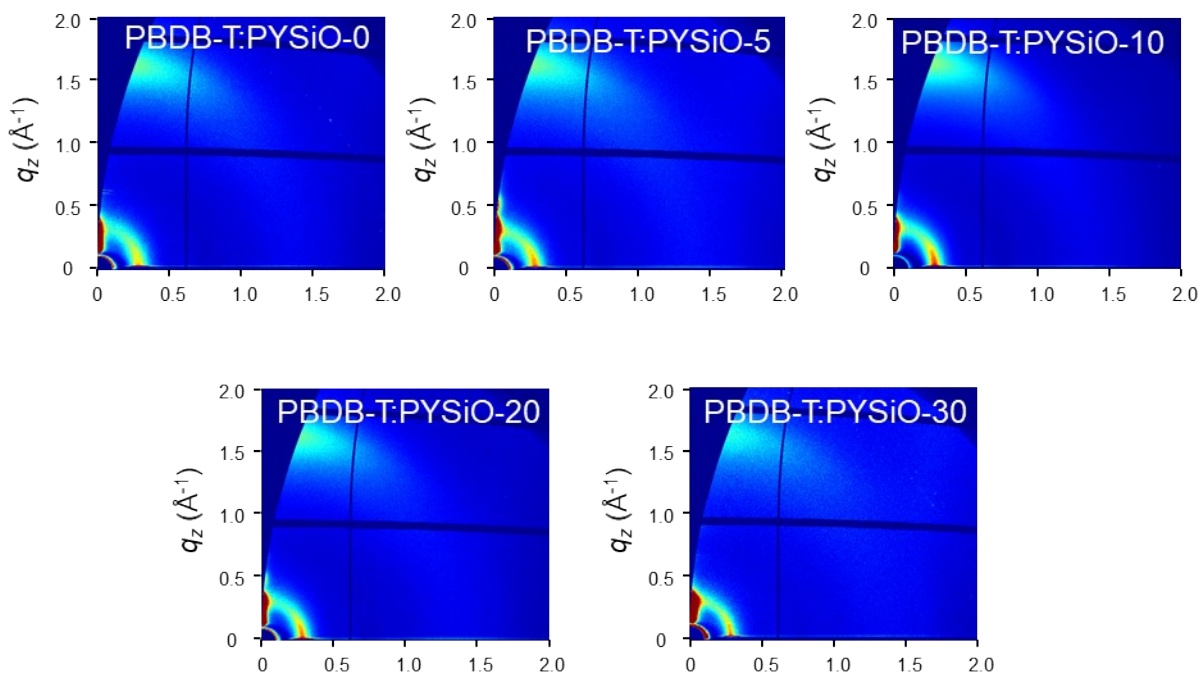


**Fig. S17.** GIXS 2D-images of PBDB-T: $P_A$ s blends.

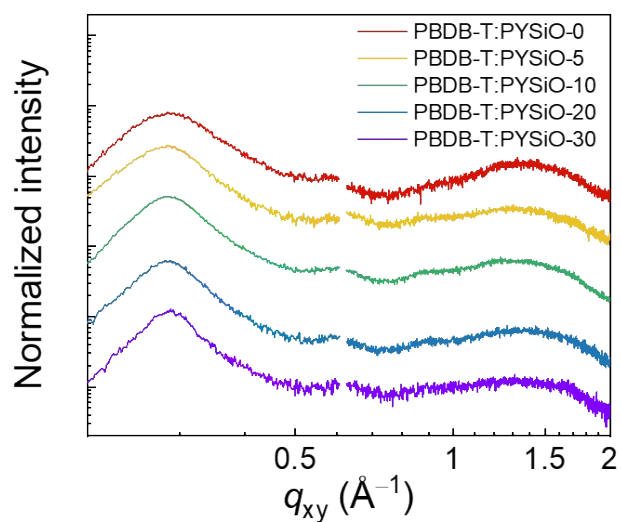


**Fig. S18.** GIXS linecut profiles of PBDB-T: $P_A$  blends in the IP direction.

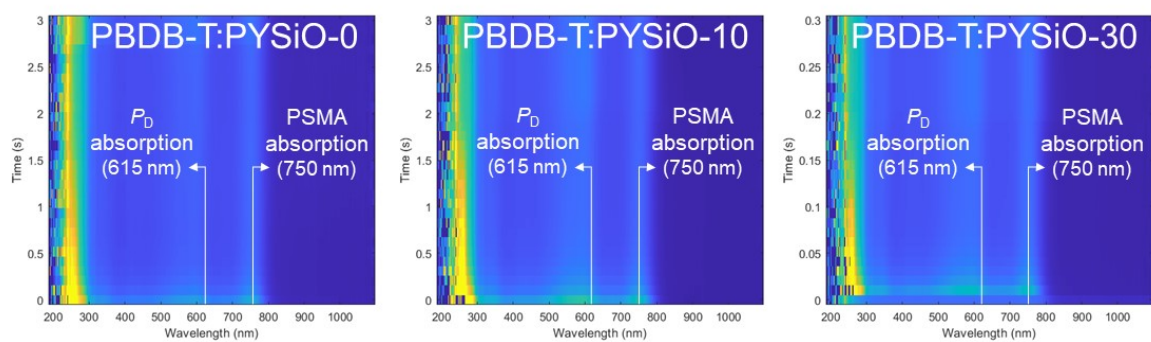


**Fig. S19.** 2D-images of *in-situ* UV-Vis profiles.

## References

1. Q. Wu, W. Wang, T. Wang, R. Sun, J. Guo, Y. Wu, X. C. Jiao, C. J. Brabec, Y. F. Li and J. Min, *Sci. China Chem.*, 2020, **63**, 1449-1460.
2. S. Q. Zhang, Y. P. Qin, J. Zhu and J. H. Hou, *Adv. Mater.*, 2018, **30**, 1800868.
3. J. Yao, B. B. Qiu, Z. G. Zhang, L. W. Xue, R. Wang, C. F. Zhang, S. S. Chen, Q. J. Zhou, C. K. Sun, C. Yang, M. Xiao, L. Meng and Y. F. Li, *Nat. Commun.*, 2020, **11**, 2726.
4. T. Kim, J. H. Kim, T. E. Kang, C. Lee, H. Kang, M. Shin, C. Wang, B. W. Ma, U. Jeong, T. S. Kim and B. J. Kim, *Nat. Commun.*, 2015, **6**, 8547.
5. J. Choi, W. Kim, S. Kim, T. S. Kim and B. J. Kim, *Chem. Mater.*, 2019, **31**, 9057-9069.
6. W. Lee, J. H. Kim, T. Kim, S. Kim, C. Lee, J. S. Kim, H. Ahn, T. S. Kim and B. J. Kim, *J. Mater. Chem. A*, 2018, **6**, 4494-4503.
7. B. J. Lin, L. Zhang, H. Zhao, X. B. Xu, K. Zhou, S. Zhang, L. Gou, B. B. Fan, L. Zhang, H. P. Yan, X. D. Gu, L. Ying, F. Huang, Y. Cao and W. Ma, *Nano Energy*, 2019, **59**, 277-284.
8. M. Xu, D. Zhang, Z. Wang, Z. Liu, X. Gao, J. He, Y. Gao, Z. Li and M. Shao, *Chem. Eng. J.*, 2022, **440**, 135829.
9. Q. P. Fan, W. Y. Su, S. S. Chen, W. Kim, X. B. Chen, B. Lee, T. Liu, U. A. Mendez-Romero, R. J. Ma, T. Yang, W. L. Zhuang, Y. Li, Y. W. Li, T. S. Kim, L. T. Hou, C. Yang, H. Yan, D. H. Yu and E. G. Wang, *Joule*, 2020, **4**, 658-672.
10. J. W. Lee, C. Sun, B. S. Ma, H. J. Kim, C. Wang, J. M. Ryu, C. Lim, T. S. Kim, Y. H. Kim, S. K. Kwon and B. J. Kim, *Adv. Energy Mater.*, 2021, **11**, 2003367.
11. Q. Wu, W. Wang, Y. Wu, R. Sun, J. Guo, M. M. Shi and J. Min, *Natl. Sci. Rev.*, 2022, **9**, nwab151.
12. Z. Genene, J.-W. Lee, S. W. Lee, Q. Chen, Z. Tan, B. A. Abdulahi, D. Yu, T. S. Kim, B. J. Kim and E. Wang, *Adv. Mater.*, 2022, **34**, 2107361.
13. Q. Wu, W. Wang, Y. Wu, Z. Chen, J. Guo, R. Sun, J. Guo, Y. Yang and J. Min, *Adv. Funct. Mater.*, 2021, **31**, 2010411.